Radiative thermalization in semiclassical simulations of light-matter interaction

Esteban D. Gadea,[1,*] Carlos M. Bustamante,[1] Tchavdar N. Todorov,[2] and Damián A. Scherlis[1]

[1]*Departamento de Química Inorgánica, Analítica y Química Física/INQUIMAE, Facultad de Ciencias Exactas y Naturales, Universidad de Buenos Aires, Buenos Aires C1428EHA, Argentina*

[2]*Atomistic Simulation Centre, School of Mathematics and Physics, Queen's University Belfast, Belfast BT7 1NN, United Kingdom*

(Received 30 September 2021; revised 25 January 2022; accepted 15 March 2022; published 1 April 2022)

Prediction of the equilibrium populations in quantum dynamics simulations of molecules exposed to black-body radiation has proved challenging for semiclassical treatments, with the usual Ehrenfest and Maxwell-Bloch methods exhibiting serious failures. In this context, we explore the behavior of a recently introduced semiclassical model of light-matter interaction derived from a dissipative Lagrangian [C. M. Bustamante, E. D. Gadea, A. Horsfield, T. N. Todorov, M. C. González Lebrero, and D. A. Scherlis, Phys. Rev. Lett. **126**, 087401 (2021)]. It is shown that this model reproduces the Boltzmann populations for two-level systems, predicting the black-body spectra in approximate agreement with Planck's distribution. In multilevel systems, small deviations from the expected occupations are seen beyond the first excited level. By averaging over fast oscillations, a rate equation is derived from the dissipative equation of motion that makes it possible to rationalize these deviations. Importantly, it enables us to conclude that this model will produce the correct equilibrium populations provided the occupations of the lowest levels remain close to unity, a condition satisfied at low temperature or small excitations.

DOI: 10.1103/PhysRevA.105.042201

I. INTRODUCTION

The ability of an electrodynamics approach to capture the equilibrium quantum populations of electrons subject to a radiation bath, in accordance with Planck's law of black-body radiation, is a fundamental feature that can be regarded as a key test to assess the overall quality of a given theoretical model of light-matter interaction [1]. A number of such models have been proposed in the framework of quantum electrodynamics, with a quantized description of both the electron and the photon degrees of freedom [2–6]. The enormous numerical demand associated with the representation of a quantum-mechanical electromagnetic field, however, enforces the use of truncations or approximations and limits the applicability of these strategies to very few electrons and photon modes. Interestingly, authors such as Boyer or Rashkovskiy have shown that thermal radiation can be entirely described within the context of classical physics without quantum assumptions, for example, including electromagnetic zero-point radiation in relativistic classical electrodynamics [7,8], or with the augmentation of the Schrödinger equation in the form of a nonlinear wave-equation [9,10].

In this work, we are interested in the semiclassical description of the light-matter interaction, which likely provides the most convenient trade-off between accuracy and efficiency to model the photophysics of atoms, molecules, and materials outside the strong photon-electron coupling regime [11]. In the realm of semiclassical approaches to the electron-radiation interaction, the former are modeled quantum mechanically while the latter is treated as a classical field. The most prominent examples of semiclassical schemes are the Ehrenfest method [12] and the Maxwell-Bloch or, more generally, the Maxwell-Liouville equations [13–17].

Very recently, we have proposed a distinct semiclassical approach that considers the electromagnetic radiation of the electron charge density as originating from a classical dipole, allowing for a first-principles Lagrangian derivation of a dissipative equation of motion where emission is cast in closed form as a unitary single-electron theory [18]. This formalism, which is directly suitable for *ab initio* implementations, quantitatively reproduces a number of experimental observations including decay rates, natural broadening, and absorption intensities. In the context of time-dependent density functional theory simulations, it yielded excited state lifetimes in atoms and ions with an accuracy within the error of experiments [18]. Here we investigate its performance in the description of thermal electromagnetic radiation. This problem has been addressed in two-level systems by Chen, Nitzan, and Subotnik in a recent communication examining the thermodynamic detailed balance with different semiclassical treatments [1]. More specifically, they studied the electronic populations produced by the Maxwell-Bloch, the Ehrenfest, and the Ehrenfest+R methods, to benchmark these three approaches according to their capability to reproduce the Boltzmann distribution. The Ehrenfest+R methodology is an *ad hoc* modification to Ehrenfest electron-photon dynamics that introduces a relaxation term to accelerate the decay rate in agreement with spontaneous emission [19]. In Ref. [1], the authors see that, among all three, it is only this heuristically amended Ehrenfest scheme that predicts the correct quantum populations in a two-level system in a radiation bath.

*egadea@qi.fcen.uba.ar

In the present article we conduct a similar analysis to explore the behavior of our dissipative equation of motion. We find that it closely approximates the Planck radiation law, in the form of Rashkovskiy's distribution [10]. We show, further, that the two schemes correspond to the same radiation field, in two different gauges. Inasmuch as Rashkovskiy's radiation field corresponds to the radiation-reaction force, we infer that radiation reaction is responsible for most of the Planck distribution, the remaining piece coming from vacuum fluctuations or charge-field correlations, depending on one's point of view.

For multilevel systems, our treatment recovers the Boltzmann distribution for the lowest electronic states, with deviations appearing at very high temperatures in the most energetic levels. We derive the rate equations for our model, which explain the origin of these deviations and enable us to visualize the assets and limitations of our radiative scheme.

II. METHODOLOGICAL PRELIMINARIES

Throughout this study, we consider a one-dimensional tight-binding (TB) model of M sites and a chosen number of electrons, with M implicit orthonormal basis functions (one per atom). Interactions are limited to first neighbors, with Hamiltonian matrix elements defined as $H_{ij} = \beta$ if $i = j \pm 1$ and $H_{ij} = 0$ in any other case, where β is the hopping parameter. (The sole exception to this rule is made in the case of the 12-level system, where second-neighbor interactions are added to break the degeneracies between energy-level spacings.) In this representation the position operator matrix is diagonal, with elements given by the interatomic distances $l, X_{ij} = l \times (i - \frac{M+1}{2})$ if $i = j$, and $X_{ij} = 0$ otherwise.

The density matrix is evolved in time according to the semiclassical dissipative equation of motion, truncated at first order, introduced in Ref. [18]:

$$\hbar\frac{\partial\hat{\rho}}{\partial t} = -i[\hat{H},\hat{\rho}] - \frac{\mu_0}{6\pi\hbar c}\ddot{\mu}[[\hat{\mu},\hat{H}],\hat{\rho}] + i[\hat{\mu}E(t),\hat{\rho}], \quad (1)$$

where μ is the dipole moment, c the speed of light, and μ_0 the magnetic permeability. The last term on the right accounts for the incoming electric field $E(t)$, which represents a frequency continuum modeled with a superposition of N single-frequency waves with randomly generated phases:

$$E(t) = \sum_{j=1}^{N} E_0(\omega_j)\cos(\omega_j t + 2\pi u_j). \quad (2)$$

Here u_j is a uniformly distributed random number, $u_j \in (0, 1]$. A constant separation between frequencies, $\Delta\omega = \omega_{j+1} - \omega_j$, was implemented in the sum, so that $\omega_j = j\Delta\omega$. A convenient way to express the magnitude of $\Delta\omega$ is in units of the peak width $\gamma = \frac{2\omega_0^3}{3\hbar c^3}l^2$. Both the values of $\Delta\omega$ and N were checked for convergence with respect to the equilibrium population of an irradiated two-level system (with energy gap $\hbar\omega_0$), finding that $\Delta\omega = \gamma$ and $N = 1.3\frac{\omega_0}{\Delta\omega}$ were good enough for the purpose of modeling continuum radiation. Regarding the dependence of E_0 on the frequency, the incoming field can be chosen to simulate black-body radiation according to Planck's law,

$$U(\omega) = \frac{\hbar\omega^3}{\pi^2c^3}\frac{1}{\exp(\frac{\hbar\omega}{kT}) - 1}, \quad (3)$$

where $U(\omega)$ is the energy density. In the case of the discrete representation of the field in Eq. (2), the energy density can be related to the amplitude of the polarized monochromatic waves as follows:

$$U(\omega) = \frac{3}{2}\frac{\epsilon_0}{\Delta\omega}E_0^2(\omega). \quad (4)$$

Owing to the oscillatory behavior of the system in the stationary state, all properties must be extracted as time-averaged values. Alternatively, Rashkovskiy's formula of black-body emission [10] was also considered:

$$U(\omega) = \frac{\hbar\omega^3}{\pi^2c^3}\frac{1}{\left[\exp\left(\frac{\hbar\omega}{kT}\right) - 1\right]\left[\exp\left(-\frac{\hbar\omega}{kT}\right) + 1\right]}. \quad (5)$$

It must be noted that, at variance with other semiclassical methods as Ehrenfest or Maxwell-Bloch, the present model does not require the explicit computation and propagation of the emitted field. This feature may become an advantage for certain applications where the focus is on the matter system.

III. RESULTS

A. Thermalization of two-level systems

A set of six different two-level systems, each with a single electron and energy gaps $\hbar\omega_0$ from 2 to 7 kT with $T = 60\,000$ K, were thermalized at this temperature using an electric field as defined in Eq. (2). To achieve this, for a given frequency, different simulations were performed varying the magnitude of E_0, seeking to reproduce the theoretical Boltzmann distribution at the target temperature, i.e., $\rho_{22} = \exp(-\frac{\hbar\omega_0}{kT})/[1 + \exp(-\frac{\hbar\omega_0}{kT})]$. From the value of E_0 found for each case, the energy density can be computed according to Eq. (4). An analytical relation between the excited-state population ρ_{22} and the field amplitude can be obtained from the combination of Eqs. (4) and (5),

$$E_0^2(\omega) = \frac{2}{3}\frac{\hbar\omega^3\Delta\omega}{\pi^2c^3\epsilon_0}\left[\frac{1}{1 - \exp\left(-\frac{\hbar\omega}{kT}\right)}\right]\rho_{22}. \quad (6)$$

In practice, it turns out to be equivalent to obtain E_0 from the simulations or from the formula above. In our simulations the field has a random component in the phase so that the agreement with the formula is observed upon time-averaging.

Figure 1 displays the time-dependent occupancies resulting from these simulations. It can be seen that the populations thermalize after about 600 fs, exhibiting fast oscillations associated with the random phases of the applied field. The spectral energy density obtained from this analysis is presented in Fig. 2, where each data point corresponds to the field required to induce an electronic population consistent with the theoretical occupation at 60 000 K. These results are confronted with the profiles arising from Planck's and Rashkovskiy's formulas.

It is observed that the simulations reproduce the qualitative features of black-body radiation, exhibiting a high accuracy for the highest frequencies. As the energy gap in the two-level

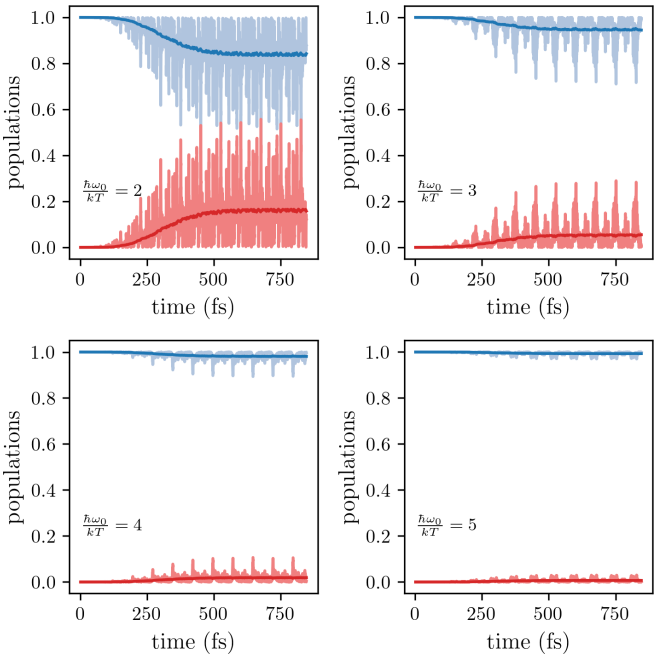

FIG. 1. Occupations as a function of time in two-level systems of characteristic frequencies 2, 3, 4, and 5 $kT/\hbar$, evolved according to the equation of motion (1), while illuminated with a continuum electromagnetic field. This field was adjusted to reproduce in each case the occupations corresponding to the Boltzmann distribution at 60 000 K. The strong oscillatory behavior reflects the random phases of the incoming light. The thick lines depict the response averaged over the fast oscillations.

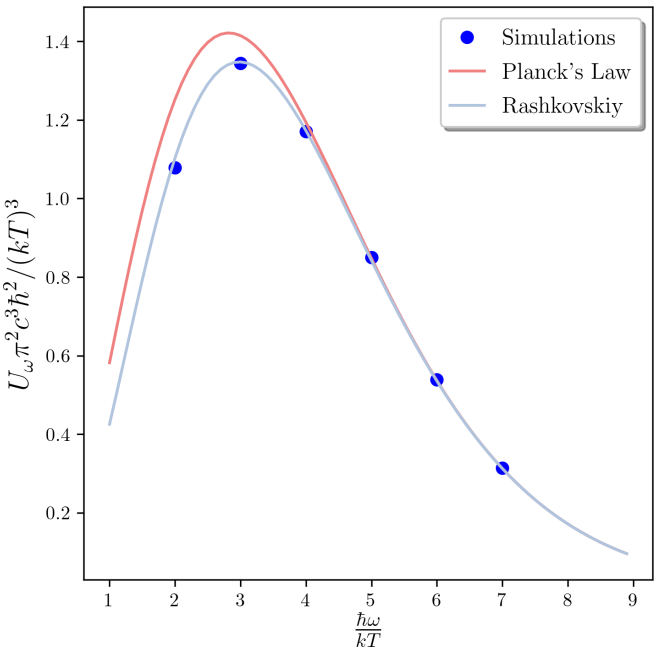

FIG. 2. Emission from a set of two level-systems thermalized with a continuum electromagnetic field at 60 000 K, obtained from time-dependent simulations with Eq. (1) (blue dots). The black-body spectra expected from Planck's law and from Rashkovskiy's expression are also shown.

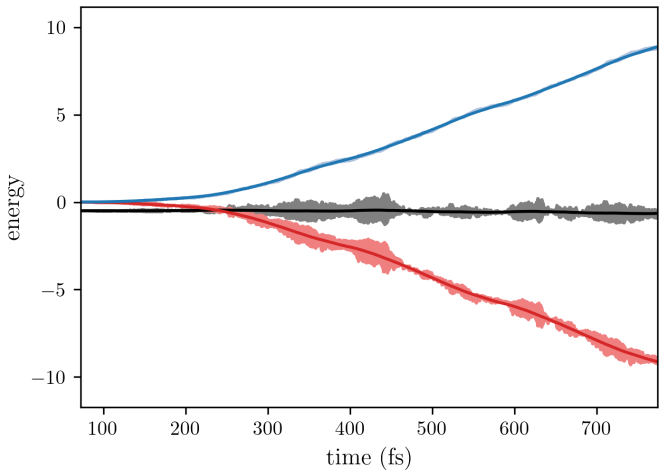

FIG. 3. Emitted (blue) and absorbed (red) energy as a function of time for a two-level system irradiated with an external field. The black line shows the sum of these two contributions plus the electronic energy. Thick lines represent for each case the average over the fast oscillations.

system approaches kT; however, the prediction becomes less accurate with respect to Planck's law. In that regime, our results are in line with those of the Rashkovskiy case.

Energy conservation can be verified in thermal equilibrium if both the power absorbed and the power dissipated are integrated in time and summed to the electronic energy. The calculation of the radiated power is straightforward from the second derivative of the dipole moment using the Larmor formula [18], whereas the rate of energy absorbed from the external field can be calculated as

$$P_{\text{abs}} = \frac{d\langle\hat{H}\rangle}{dt} = \frac{1}{i\hbar}\langle[\hat{H}, \hat{\mu}E(t) + \hat{H}]\rangle$$
$$= -\frac{E(t)}{i\hbar}\text{Tr}(\hat{\rho}[\hat{\mu}, \hat{H}]), \tag{7}$$

where it was assumed that the dissipation does not affect the rate of energy absorbed. Figure 3 displays the temporal evolution of the emitted and absorbed energies computed as the integrals of the corresponding powers, for a two-level system subject to the incoming radiation. The thick lines represent the average over the fast oscillations. There is a transient of nearly 250 fs before the system thermalizes and reaches a stationary state. The black line depicts the sum of these two contributions plus the electronic energy. It can be seen that, beyond the fast oscillations, the energy is conserved throughout the simulation.

B. Thermalization of multilevel systems

Employing the equation of motion (1), a four-level system with one electron was illuminated and equilibrated with black-body radiation, or, more specifically, with a continuum of electromagnetic frequencies [Eq. (2)] with energy density $U(\omega)$ defined according to Planck's or to Rashkovskiy's emission spectra [Eqs. (3) and (5)] at 60 000 K, which amounts to $\hbar\omega/kT = 2.63$ [taking $\hbar\omega$ as the highest occupied molecular orbital–lowest unoccupied molecular orbital

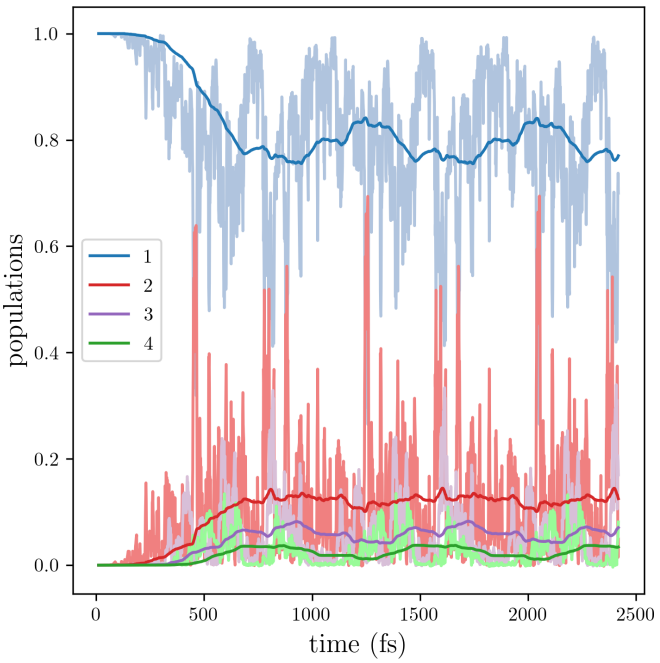

FIG. 4. Occupations as a function of time in a four-level system while illuminated with a continuum electromagnetic field at 60 000 K. The fast oscillations arising from the random phases of the incident radiation are averaged out in the thick traces.

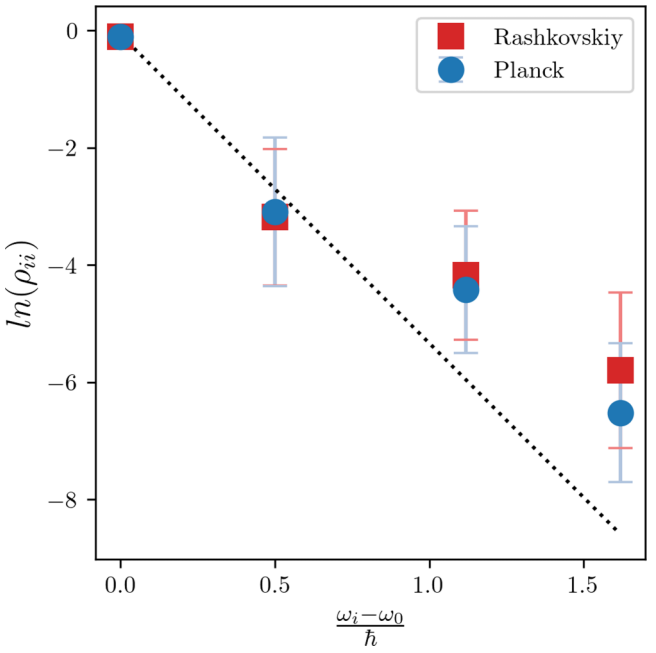

FIG. 5. Logarithm of the steady-state populations as a function of the energy, for a set of four-level systems with one electron thermalized with Planck's (blue dots) or Rashkovskiy's (red squares) black-body radiation at 60 000 K. The dotted line indicates the expected trend according to Boltzmann statistics.

(HOMO-LUMO) energy gap). Figure 4 presents the evolution of the populations with respect to time. In the case of systems with more than two levels, the electronic temperature cannot be directly assessed from the population of a single excited state. One possible way to estimate the temperature is from the (inverse of the) slope of the logarithm of the occupations plotted versus the energy of the levels. Figure 5 presents such a plot for a four-level system. Regardless of the parameters and the kind of black-body radiation used, it is found that the density distribution does not obey Boltzmann statistics; only the first two levels fall on the expected trend. The highest occupations tend to be systematically larger than the ones corresponding to 60 000 K. In considering these results it must be noted, however, that the occupations of the two highest levels are at least an order of magnitude smaller than the populations of the first excited state. In particular, the deviations manifest in the logarithmic plots of Fig. 5 are, in absolute value, no larger than 10^{-4}.

These positive deviations in the excited-state populations can be equally observed in a single-electron system of 12 levels (Fig. 6). Again, only the occupations of the ground state and the first excited state are aligned with the slope corresponding to the Boltzmann distribution at 20 000 K (the temperature of the black body used in this case, equivalent to $\hbar\omega/kT = 0.485$ if ω is the frequency associated with the HOMO-LUMO gap), whereas the rest of the data points are shifted to larger populations.

In the presence of five electrons, a shift toward larger occupations with respect to the Fermi-Dirac distribution is observed, but in this case the deviations are seen for the highest four levels, with the lowest eight remaining close to the theoretical trend. Given the small magnitude of the deviations, in a graph of the occupations as a function of the energy [Fig. 7(a)], the curve corresponding to the simulations can hardly be distinguished from the Fermi-Dirac distribution at that temperature; the deviations become evident only in the logarithmic plot [Fig. 7(b)], for energies exceeding ω_0 by more than $1.5\hbar$.

When the number of levels was increased further, simulations with many electrons exhibited additional deviations. This behavior was attributed to the degeneracies inherent to multilevel systems arising from a first-neighbor TB model, which lead to self-excitation and the stabilization of subradiant states (see discussion in the next section).

C. Rate equations

Under a few assumptions, Eq. (1) can be used to get an expression for the populations as a function of time. We treat the dissipative term and the term involving the applied field as perturbations and consider, in the interaction picture, the rates of change of the occupations of the eigenstates of the unperturbed Hamiltonian, with energies $\hbar\omega_i$. For these rates of change perturbation theory gives

$$\frac{d\rho_{jj}}{dt} = \sum_k \left[\frac{4\pi^2|\mu_{kj}|^2}{3\hbar^2}(\rho_{kk} - \rho_{jj})U(\omega_{kj}) + 2\gamma_{kj}|\rho_{jk}|^2 \right], \tag{8}$$

where $\gamma_{ij} = \frac{2\omega_{ij}^3}{3\hbar c^3}|\mu_{ij}|^2$ and we have chosen units in which $4\pi\epsilon_0 = 1$. Moreover, in the absence of a field, the derivatives of the off-diagonal elements of the density matrix take the

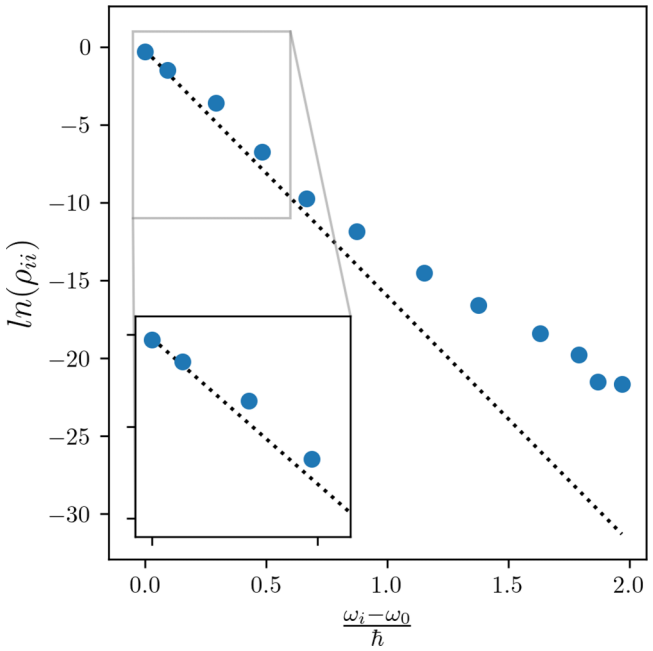

FIG. 6. Logarithm of the steady-state populations as a function of the energy, for a 12-level system with one electron thermalized with Planck's black-body radiation at 20 000 K. Simulations were based on the equation of motion (1). The dotted line indicates the expected trend according to Boltzmann statistics at that temperature.

following form:

$$\frac{d\rho_{ij}}{dt}|_{i\neq j} = \sum_k \rho_{ik}\rho_{kj}(\gamma_{ki} + \gamma_{kj}). \tag{9}$$

A full derivation of these expressions is presented in the Appendix.

We observe that these rate equations agree with those produced by the Rashkovksiy theory [10] and lead to the Rashkovskiy distribution for a two-level system. This agreement is an important reality check. The dissipative term in our theory was shown in the Supplemental Material of Ref. [18] to correspond to the vector potential in Eq. (33) therein. This vector potential produces the same electric field as that corresponding to Rashkovskiy's dissipative term, in turn equal to the radiation-reaction field corresponding to the Abraham-Lorentz force.

For two level and one electron systems, these rate equations reproduce closely the dynamics obtained by direct integration of the equation of motion (1). Figure 8 presents the temporal evolution of the energy for two different initial states.

In a four-level system, however, it can be seen that the dynamics produced by the rate equations do not relax beyond the lower level that formed the departing coherent mixture (Fig. 9), whereas the direct integration of Eq. (1) leads to the ground state through a sequence of deexcitations. In these simulations the initial state consists of a linear combination of the third and fourth eigenfunctions, with the majority component coming from the latter, thus representing an almost pure excited state (the mixture is necessary to induce dissipation in Eq. (1), see Ref. [18]). Interestingly, when a second electron is

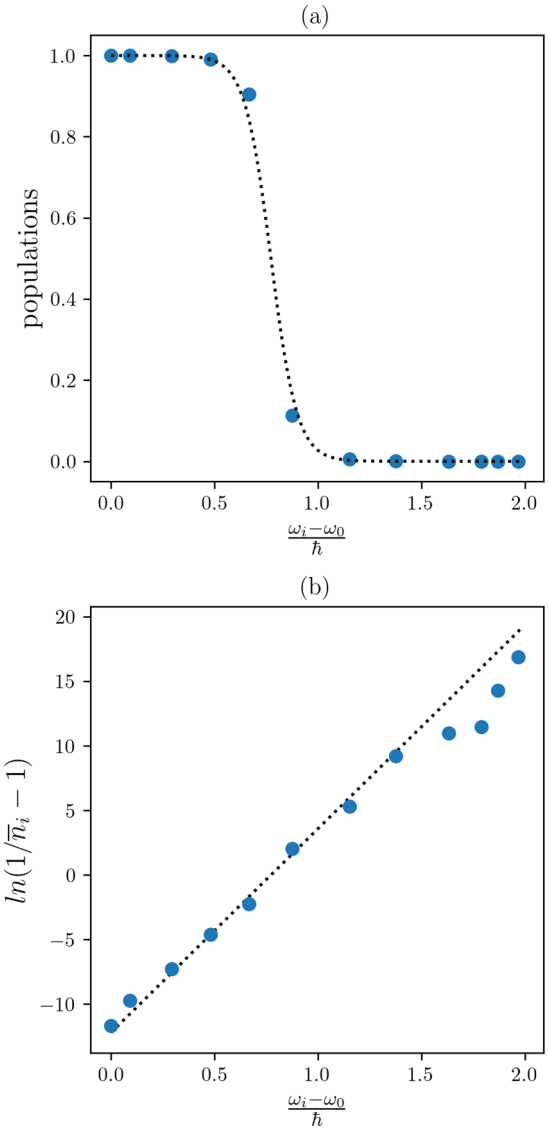

FIG. 7. Populations as a function of energy, for a 12-level system with five electrons thermalized with Planck's black-body radiation at 20 000 K are shown with blue dots. The populations corresponding to the Fermi-Dirac distribution at the same temperature are indicated with dotted lines. Direct and logarithmic plots are depicted in panels (a) and (b), respectively.

added in the lowest level, energy dissipation is stalled, as can be seen in Fig. 9(b). In the systems examined in Figs. 9(a) and 9(b) the energy gaps between levels are degenerate. When this degeneracy is broken, as in the model explored in Fig. 9(c), the equation of motion (1) recovers energy dissipation. For all three cases considered in Fig. 9, the physical evolution of the electronic state is well described by the equation of motion (1) (blue curves), as is discussed in the next section where these observations are interpreted.

IV. DISCUSSION

In the presence of a single electron in a pure state, the dissipative term in Eq. (8) can be written in terms of the

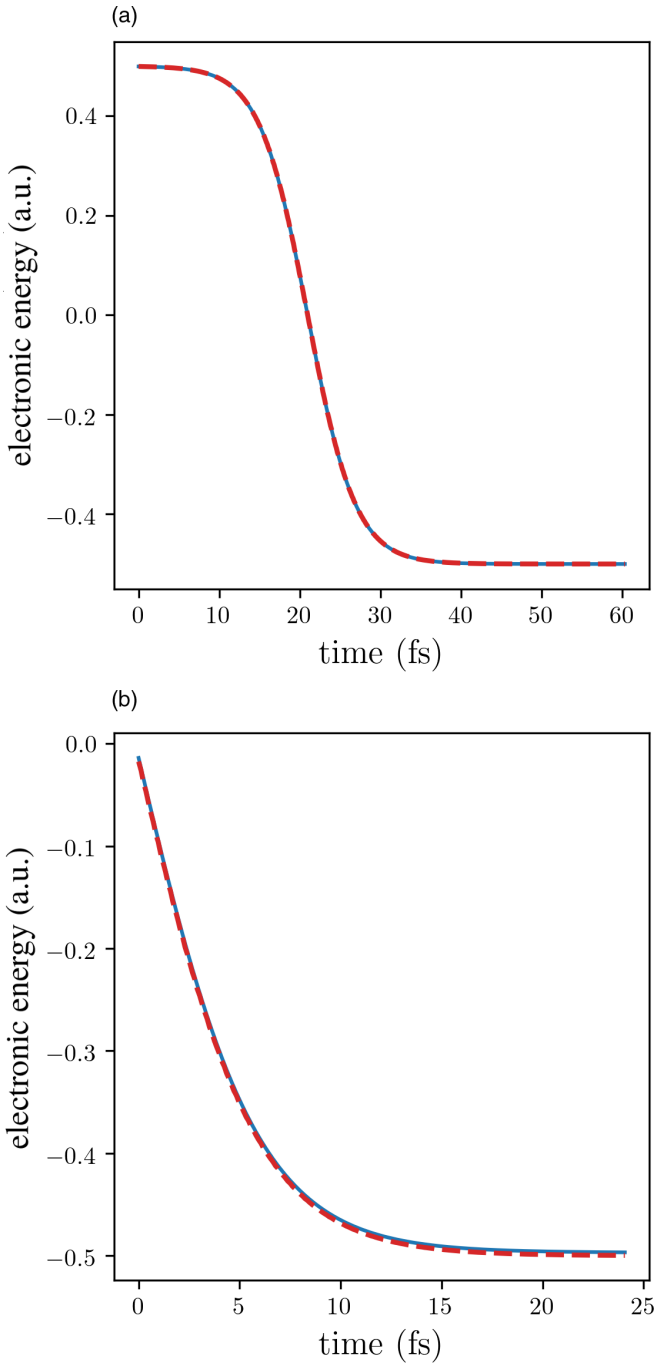

FIG. 8. Electronic energy as a function of time, for a one-electron two-level system evolved with the equation of motion (1) (blue line) and the rate equation (8) (dashed red line). (a) Initial state prepared as a coherent mixture of the two levels. (b) Initial state induced by excitation with an electric pulse.

diagonal elements of the density matrix,

$$D_{jj} = 2\sum_k \gamma_{kj}|\rho_{jk}|^2 = 2\sum_k \gamma_{kj}\rho_{jj}\rho_{kk}. \tag{10}$$

In particular, for an electron in a two-level system in the absence of an incoming field, the rate equation assumes the

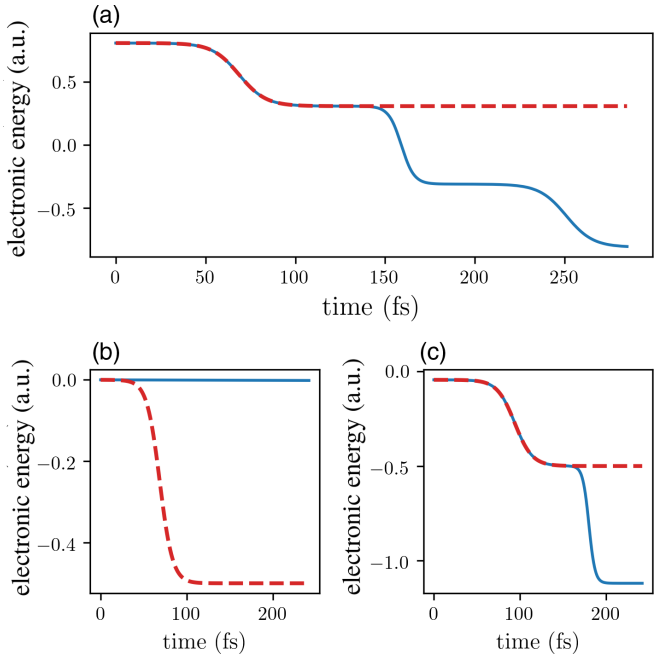

FIG. 9. Electronic energy as a function of time for four-level systems evolved with the equation of motion (1) (blue line) and the rate equation (8) (dashed red line), starting with an electron in the highest energy level. (a) One-electron system with degenerate energy gaps. (b) Two-electron system with degenerate energy gaps. (c) Two-electron system with nondegenerate energy gaps.

following form:

$$\frac{d\rho_{22}}{dt} = -\frac{d\rho_{11}}{dt} = 2\gamma_{12}\rho_{22}\rho_{11} = 2\gamma_{12}\left(\rho_{22} - \rho_{22}^2\right). \tag{11}$$

For small excitations $\rho_{11} \approx 1$, and the equation above reproduces the Fermi golden rule:

$$\frac{d\rho_{22}}{dt} \approx 2\gamma_{12}\rho_{22}. \tag{12}$$

According to this result, Eq. (1) yields exponential decays for small perturbations, while the dissipation rate is decelerated when the occupation of the excited state is significant, by virtue of the quadratic term. This behavior has, in fact, been reported in Ref. [18].

Figure 2 indicates that the field amplitude E_0 needed to reach the Boltzmann population in the two-level system is smaller than the field calculated from Planck's law. Consequently, one can expect that for a given temperature, ρ_{22} exceeds the value corresponding to the Boltzmann distribution. This is manifest in Fig. 10, which displays the excited population versus $\hbar\omega_0/kT$ as obtained from the simulations and from Eq. (6). If this system were thermalized according to Rashkovskiy's expression for black-body emission, the simulations would reproduce the Boltzmann distribution, consistently with the agreement visible in Fig. 2.

Figure 10 also includes the data from Ehrenfest simulations reported for this system in Ref. [1], showing that the overestimation is more severe in comparison with the current model, in particular, when the energy of the transition is of the order of kT. The reason why these two models predict different behaviors, and, more specifically, why one

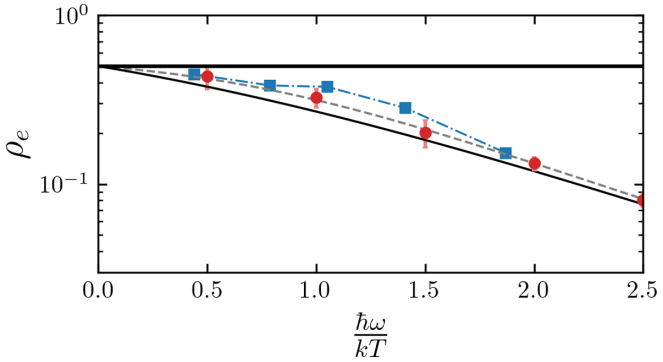

FIG. 10. Excited-state population as a function of temperature for a two-level system. The continuous curve depicts the Boltzmann distribution, the red dots show the results from the simulations using the present model, and the dashed gray line corresponds to Eq. (6). Also shown are results from Ehrenfest simulations extracted from Ref. [1] (blue squares).

seemingly outperforms the other, is not obvious to us. Even if both are mean-field semiclassical approaches based on the dipolar approximation, they address the same problem from two different perspectives. In Ehrenfest, the density oscillations are damped by virtue of the interaction with the scattered field, or a self-interaction. This self-interaction is not explicitly introduced in the dissipative equation of motion, though it may be present as the result of the "friction" in the Liouville–von Neumann equation rooted in the Larmor formula. An algebraic comparison with Ehrenfest and with the self-interaction therein is part of ongoing work.

In the case of multilevel systems with one electron, the derivative of the occupations is

$$\frac{d\rho_{jj}}{dt} = 2\sum_k \gamma_{kj}\rho_{jj}\rho_{kk}. \tag{13}$$

Again, the dynamics of the first excited state is determined by the product $\gamma_{12}\rho_{22}\rho_{11}$, plus the contribution of terms involving the populations of the higher levels, which will, in general, be negligible with respect to those of the two lowest states except for high temperatures. In this way, the decay from the first excited state will still be mostly exponential. On the other hand, the occupancy of this first excited state will enter the dynamics of the third and higher levels.

It can be seen from Eq. (11) [and also from Eq. (13)] that when a given level becomes fully populated (i.e., $\rho_{jj} \approx 1$ and $\rho_{kk} \approx 0$ for all $k \neq j$), its time derivative goes to zero and emission is quenched. This explains the results illustrated in Fig. 9(a). The integration of the original model, the equation of motion (1), does not suffer from this artifact, thanks to the terms that couple nonresonant frequencies and that are able to destabilize pure or close-to-pure states. These terms coupling fluctuations of different frequencies are eliminated when the fast oscillations are averaged out.

The lack of dissipation observed for our model in the case of two electrons in the four-level system of Fig. 9(b) can be interpreted with the assistance of Fig. 11(a), which presents the occupancies as a function of time for this system. Here, the degeneracy between all the accessible transitions provokes the self-excitation of the molecule: the decay from

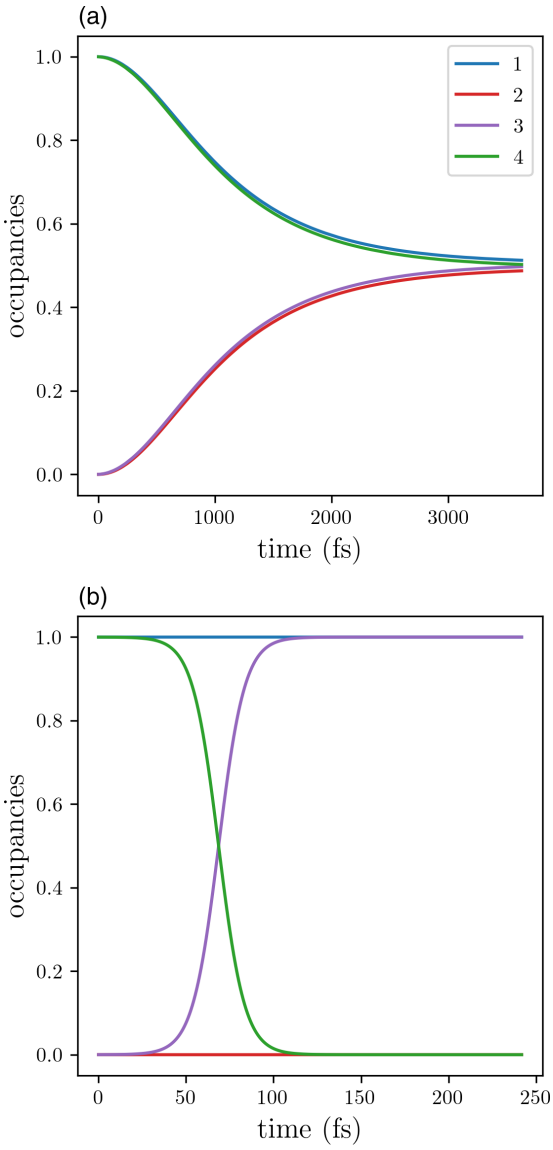

FIG. 11. Populations as a function of time in a four-level system with two electrons and degenerate gaps. In the initial state, the electrons occupy the lowest and highest levels, respectively. (a) Evolution according to the equation of motion (1). (b) Evolution according to the rate equation (8).

level 4 to level 3 induces the promotion of the other electron from the first level to the second level. In this way the system evolves to a stationary state where all four levels are partially occupied and where the individual dipoles of each particle resonate in counterphase, canceling each other to switch off energy dissipation. The dynamics remains trapped in this state without emitting for the whole length of the simulation, provided that it is not perturbed. This kind of behavior in which the system equilibrates in an excited state storing optical energy has been characterized in the literature as "limited superradiance" or "subradiance" [20]. Not long ago, this elusive phenomenon was experimentally measured in cold-atom samples [21]. Its occurrence in nature is not readily observable because it is the outcome of a delicate equilibrium which is easily deactivated through thermal coupling or other decoherence processes associated with the environment. The fast

oscillations seem to play a role in stabilizing this state, since it is not captured by the simpler rate equation [Fig. 11(b)]. In this case the electron in the highest level relaxes to the next one down, to remain trapped there as already seen for the single-electron example of Fig. 9(a). When the degeneracy is broken [Fig. 9(c)], the subradiance effect is destroyed and our model predicts the expected cascade.

It is interesting to note that in the context of the Dicke model, subradiance can be represented through the construction of Lindblad dissipators and the population of the so-called dark states of the Hamiltonian, which are characterized by their inability to decay through a collective interaction [22–24]. Our semiclassical Hamiltonian captures the same effect thanks to the dynamical coupling of the dipoles of the fluctuating electronic charges. The case study proposed by Piñeiro Orioli and Rey [24] provides a nice example to compare these two descriptions, based on the dark states and on the semiclassical emission, respectively. Those authors considered in that work a lattice of two-level systems with two fermionic particles per site. In their simplest model, a single lattice site with an internal level structure consisting of two-degenerate ground states and two-degenerate excited states, there is only one dark state [24]. In the framework of our tight-binding electronic Hamiltonian, such a dark-state can be identified with a two-level system of two electrons in the singlet state (with spin $1/2$ and $-1/2$, respectively) with one particle in the ground state and the other one excited. In analogy with the quantum Dicke model analyzed in Ref. [24], the evolution of our two-electron system leads to a subradiant solution where both particles remain trapped in a partially excited state, and in which the dipole moments of the two particles interfere destructively. These two treatments can thus be regarded as two sides of the same coin. Further investigations on the induction of subradiant and superradiant states with the present model are in progress [25].

The first term on the right-hand side in Eq. (8) accounts for the incoming radiation. In thermal equilibrium, this term has to be equal to the dissipation rate,

$$D_{jj} = -\sum_k \frac{4\pi^2|\mu_{kj}|^2}{3\hbar^2}(\rho_{kk} - \rho_{jj})U(\omega_{kj}). \tag{14}$$

At the same time, $U(\omega)$ must be given by Planck's law [Eq. (3)], and the populations must follow the Boltzmann distribution, $\rho_{nn} = \exp(-\frac{\hbar\omega_n}{kT})/Z$. Then, from Eq. (14) it is possible to write

$$D_{jj} = -\sum_k \frac{4|\mu_{kj}|^2|\omega_{jk}|^3}{3\hbar c^3}\frac{1}{\exp\left(\frac{\hbar|\omega_{jk}|}{kT}\right)-1} \times\left[\exp\left(-\frac{\hbar\omega_k}{kT}\right) - \exp\left(-\frac{\hbar\omega_j}{kT}\right)\right]\frac{1}{Z}, \tag{15}$$

which after some algebra yields

$$D_{jj} = 2\sum_{k<j}\gamma_{kj}\rho_{jj} + 2\sum_{k>j}\gamma_{kj}\rho_{kk}. \tag{16}$$

At low temperatures, when $\rho_{11} \approx 1$ and $\rho_{jj} \gg \rho_{j+1,j+1}$, the leading term for the first excited state in this expression will be consistent with the prediction of the rate equation under these conditions [Eq. (13)],

$$D_{22} \approx \gamma_{12}\rho_{22}\rho_{11} \approx \gamma_{12}\rho_{22}. \tag{17}$$

Alternatively, in many-electron extended systems the Fermi-Dirac distribution can be considered,

$$\rho_{nn} = \frac{1}{\exp\left(\frac{\hbar\omega_n-\mu}{kT}\right)+1}, \tag{18}$$

in which case Eq. (14) adopts the following form:

$$D_{jj} = -\sum_k \frac{4|\mu_{kj}|^2|\omega_{jk}|^3}{3\hbar c^3}\frac{1}{\exp\left(\frac{\hbar|\omega_{jk}|}{kT}\right)-1} \times\left(\frac{1}{\exp\left(\frac{\hbar\omega_k}{kT}-\mu\right)+1} - \frac{1}{\exp\left(\frac{\hbar\omega_j}{kT}-\mu\right)+1}\right), \tag{19}$$

with μ being the Fermi level. Expression (19) can be further rearranged to give

$$D_{jj} = 2\sum_{k<j}\gamma_{kj}\rho_{jj}(1-\rho_{kk}) + 2\sum_{k>j}\gamma_{kj}\rho_{kk}(1-\rho_{jj}). \tag{20}$$

In this case only those terms involving partially filled levels close to the Fermi energy will contribute to the dissipative dynamics.

V. SUMMARY

This work scrutinizes the performance of a recent semiclassical formalism for dissipative electron dynamics [18] to model black-body thermal equilibrium. To this end, tight-binding simulations were conducted in 2-, 4-, and 12-level systems of one or more electrons thermalized with electromagnetic radiation. For 2-level systems the model reproduces the Boltzmann populations corresponding to the incident radiation temperature and quantitatively predicts Planck's black-body spectra with an accuracy that becomes better the higher the frequencies, e.g., $\hbar\omega > 4\ kT$. This result is remarkable as far as no other parameter-free semiclassical approaches have been shown to recover the correct distribution in thermal equilibrium [1]. For multilevel systems, the model still provides the right populations of the two lowest levels, but is less accurate for the rest. Electron dynamics simulations initiated from an excited state exhibit the expected cascadewise relaxation in which the accessible levels are consecutively populated in decreasing order. Interestingly, in many-electron systems with degenerate energy gaps, this cascade is interrupted by the emergence of a steady state where emission ceases and electron levels remain partially filled. This phenomenon, which is the consequence of the self-excitation of the lowest-energy electrons and has been termed "subradiance" in the theoretical literature [20], was recently detected experimentally in an atomic cloud [21].

The dependence of the populations as a function of time was derived analytically from the dissipative equation of motion by a perturbative argument. The rate equations obtained in this way for one-electron systems indicate that the radiative dynamics will follow FGR when the occupancy of the ground-state level is not too different from unity, explaining why the agreement is better for low temperatures and why Planck's black-body emission spectrum is more accurately described in the high-frequency region. Hence, these rate equations suggest that the present semiclassical model will be less reliable at very high temperatures or in certain situations

far from equilibrium, as in the case of population inversion. Moreover, the comparison of the simulations based on the rate equations and on the original model evinces the importance of the fast oscillations in the deexcitation dynamics, through the coupling of nonresonant modes. The dynamics arising from the rate equations will coincide with that of Eq. (1) provided that the fast oscillations, which are averaged out in the derivation of the former, are not determinant. These fast oscillations are important to induce relaxation from intermediate levels during a cascade. They are also relevant to couple the individual dipoles in degenerate transitions that lead to subradiant states in multielectron systems. Therefore, the descriptions will differ for cascades in multistate structures but also for an ensemble of 2-level systems exhibiting degenerate states.

We have, finally, demonstrated the close connection of the present theory to that of Rashkovskiy [10]. We have argued that this is because the two describe the same radiation field in two different gauges. The conclusion is that the radiation self-force that they capture (the Abraham-Lorentz force) leads to the Rashkovskiy distribution, which in turn closely resembles the Planck spectrum especially at high frequencies or low temperatures. The difference between the two distributions, then, is due to the remaining ingredient of charge-field interaction, namely, the vacuum fluctuations or the charge-field correlations, depending on one's point of view.

ACKNOWLEDGMENTS

We are grateful to Andrew Horsfield and Lorenzo Stella for helpful discussions. This work has been funded by the European Union's Horizon 2020 research and innovation programme through the project ATLANTIC under Grant No. 823897. We acknowledge Agencia Nacional de Promoción Científica y Tecnológica de Argentina (Grants No. PICT 2015-2761 and No. PICT 2016-3167).

APPENDIX

The first term in Eq. (8) arises directly from Fermi's golden rule (FGR) applied to the transitions driven by $E(t)$. Indeed the net particle current from state k into state j, under interaction with a sinusoidal electric field of frequency ω and amplitude $E_0(\omega)$, according to FGR is

$$\Gamma_{k\to j} = \frac{2\pi}{\hbar^2}\frac{1}{4}(\rho_{kk}-\rho_{jj})E_0^2|\mu_{jk}|^2[\delta(\omega_{jk}+\omega)+\delta(\omega_{jk}-\omega)]. \tag{A1}$$

Now we assume that interactions with different frequencies are independent (equivalent to saying that different frequency components have uncorrelated phases and averaging over these phases) and sum over frequency components. This gives

$$\Gamma_{k\to j} = \frac{2\pi}{\hbar^2}\frac{1}{4}(\rho_{kk}-\rho_{jj})E_0^2|\mu_{jk}|^2 d(|\omega_{jk})], \tag{A2}$$

where $d(\omega)$ is the density of states for the frequency components of the field. From Eq. (4) it is given by

$$d(\omega) = \frac{2}{3\epsilon_0}\frac{U(\omega)}{E_0^2(\omega)}, \tag{A3}$$

which then gives our desired result.

On the other hand, the dissipative contribution, Eq. (9) or second term in Eq. (8), emerges directly from the radiative term in the equation of motion (1) after expanding the wave functions in an orthonormal basis and averaging over fast oscillations. More specifically, the dissipative Schrödinger equation introduced in Ref. [18] can be cast to first order as

$$i\hbar\frac{d\psi_a(\mathbf{r},t)}{dt} = \hat{H}\psi_a(\mathbf{r},t) + \frac{2\alpha}{i3c^2}\frac{d^2\langle X\rangle}{dt^2}[\hat{X},\hat{H}]\psi_a(\mathbf{r},t), \tag{A4}$$

where ψ_a are the electronic wave functions, α is the fine-structure constant, $\alpha = \frac{\mu_0 e^2 c}{4\pi\hbar}$, and e is the electron charge. If the wave functions are written in terms of an orthonormal basis set $\{u_k\}$,

$$\psi_a(\mathbf{r},t) = \sum_k c_{ak}(t)u_k(\mathbf{r})\exp(-i\omega_k t), \tag{A5}$$

it is possible to insert the last equality in Eq. (A4) to get

$$\begin{aligned} i\hbar\sum_n \frac{dc_{\rm an}}{dt}u_n(\mathbf{r})\exp(-i\omega_n t) &= \frac{2\alpha\hbar}{i3c^2}\frac{d^2\langle X\rangle}{dt^2}\sum_n\sum_k \omega_n c_{\rm an}u_k(\mathbf{r})\exp(-i\omega_n t)X_{kn} \\ &\quad - \frac{2\alpha\hbar}{i3c^2}\frac{d^2\langle X\rangle}{dt^2}\sum_n\sum_k c_{\rm an}u_k(\mathbf{r})X_{kn}\exp(-i\omega_n t)\omega_k, \end{aligned} \tag{A6}$$

where we have used $\hat{H}u_k(\mathbf{r}) = \omega_k u_k(\mathbf{r})$ and $\hat{X}u_k(\mathbf{r}) = \sum_n X_{kn}u_n(\mathbf{r})$. After multiplying both members by $u_j^*(\mathbf{r})$, and integrating over space, the time derivative of the coefficients takes the form:

$$i\hbar\frac{dc_{\rm an}}{dt} = \frac{2\alpha\hbar}{i3c^2}\sum_k c_{ak}\omega_{kn}X_{nk}\ddot{X}\exp(-i\omega_{kn}t), \tag{A7}$$

with

$$\ddot{X} = -\sum_b\sum_i\sum_j \omega_{ji}^2 c_{bi}^* c_{bj}X_{ij}\exp(-i\omega_{ji}t) \tag{A8}$$

and $\omega_{kn} = \omega_k - \omega_n$. The sum above involves products of complex exponentials, of which only those associated with the same frequency will survive when averaged over time,

$$\begin{aligned} &\langle\exp(-i\omega t)\times\exp(i\omega' t)\rangle_t \\ &\quad = \lim_{t_0\to\infty}\frac{1}{2t_0}\int_{-t_0}^{+t_0}\exp[-i(\omega-\omega')t]dt, \end{aligned} \tag{A9}$$

leading to

$$i\hbar\frac{dc_{\rm an}}{dt} \approx \frac{2i}{3c^3}\sum_b\sum_k c_{bk}^* c_{ak}c_{bn}|\mu_{nk}|^2\omega_{kn}^3 \tag{A10}$$

(here we ignore degeneracies among the energy-level spacings). The insertion of this result in the time derivative of the

density matrix elements,

$$\frac{d\rho_{ij}}{dt} = \sum_a \left\{ \frac{dc_{ai}}{dt} c^*_{aj} + \frac{dc^*_{aj}}{dt} c_{ai} \right\}, \tag{A11}$$

produces the final outcome:

$$\frac{d\rho_{ij}}{dt} = \sum_k \rho_{ik}\rho_{kj} \frac{2\omega^3_{ki}}{3\hbar c^3} |\mu_{ki}|^2 + \sum_k \rho_{kj}\rho_{ik} \frac{2\omega^3_{kj}}{3\hbar c^3} |\mu_{kj}|^2. \tag{A12}$$

[1] H.-T. Chen, T. E. Li, A. Nitzan, and J. E. Subotnik, Phys. Rev. A **100**, 010101(R) (2019).

[2] M. Ruggenthaler, F. Mackenroth, and D. Bauer, Phys. Rev. A **84**, 042107 (2011).

[3] M. Ruggenthaler, J. Flick, C. Pellegrini, H. Appel, I. V. Tokatly, and A. Rubio, Phys. Rev. A **90**, 012508 (2014).

[4] I. V. Tokatly, Phys. Rev. Lett. **110**, 233001 (2013).

[5] C. Pellegrini, J. Flick, I. V. Tokatly, H. Appel, and A. Rubio, Phys. Rev. Lett. **115**, 093001 (2015).

[6] M. Sánchez-Barquilla, R. E. F. Silva, and J. Feist, J. Chem. Phys. **152**, 034108 (2020).

[7] T. H. Boyer, Phys. Rev. **182**, 1374 (1969).

[8] T. H. Boyer, Am. J. Phys. **86**, 495 (2018).

[9] S. A. Rashkovskiy, Indian J. Phys. **91**, 607 (2017).

[10] S. A. Rashkovskiy, Indian J. Phys. **92**, 289 (2018).

[11] J. Flick, M. Ruggenthaler, H. Appel, and A. Rubio, Proc. Natl. Acad. Sci. USA **114**, 3026 (2017).

[12] T. E. Li, A. Nitzan, M. Sukharev, T. Martinez, H.-T. Chen, and J. E. Subotnik, Phys. Rev. A **97**, 032105 (2018).

[13] A. Fratalocchi, C. Conti, and G. Ruocco, Phys. Rev. A **78**, 013806 (2008).

[14] M. Sukharev and A. Nitzan, Phys. Rev. A **84**, 043802 (2011).

[15] Y. Li, S. He, A. Russakoff, and K. Varga, Phys. Rev. E **94**, 023314 (2016).

[16] D. J. Trivedi, D. Wang, T. W. Odom, and G. C. Schatz, Phys. Rev. A **96**, 053825 (2017).

[17] S. Yamada, M. Noda, K. Nobusada, and K. Yabana, Phys. Rev. B **98**, 245147 (2018).

[18] C. M. Bustamante, E. D. Gadea, A. Horsfield, T. N. Todorov, M. C. González Lebrero, and D. A. Scherlis, Phys. Rev. Lett. **126**, 087401 (2021).

[19] H.-T. Chen, T. E. Li, M. Sukharev, A. Nitzan, and J. E. Subotnik, J. Chem. Phys. **150**, 044102 (2019).

[20] M. Gross and S. Haroche, Phys. Rep. **93**, 301 (1982).

[21] W. Guerin, M. O. Araújo, and R. Kaiser, Phys. Rev. Lett. **116**, 083601 (2016).

[22] M. Gegg, A. Carmele, A. Knorr, and M. Richter, New J. Phys. **20**, 013006 (2018).

[23] E. Frishman and M. Shapiro, Phys. Rev. Lett. **87**, 253001 (2001).

[24] A. Piñeiro Orioli and A. M. Rey, Phys. Rev. Lett. **123**, 223601 (2019).

[25] C. Bustamante, E. Gadea, T. N. Todorov, and D. A. Scherlis, (unpublished).